Wideband SIW Horn Antenna with phase correction for New Generation Beam Streerable Arrays

Paola, Carla di; Zhao, Kun; Zhang, Shuai; Pedersen, Gert Frølund

Published in:
2019 IEEE 90th Vehicular Technology Conference (VTC2019-Fall)

DOI (link to publication from Publisher):
10.1109/VTCFall.2019.8891322

Publication date:
2019

Document Version
Accepted author manuscript, peer reviewed version

Wideband SIW Horn Antenna with phase correction for New Generation Beam Streerable Arrays

Carla Di Paola[1], Kun Zhao[1,2], Shuai Zhang[1], Gert Frølund Pedersen[1]
[1]Department of Electronic Systems, Aalborg University, Denmark, {cdp, kz, sz, gfp}@es.aau.dk
[2]Research Center Lund, Sony Corporation, Lund, Sweden

***Abstract*—This paper presents a new SIW horn antenna with high performance in the mm-wave bands for the next generation mobile devices. The proposed antenna is integrated in a double layer of Rogers RO4003C substrate and requires a clearance of only 3 mm. Air vias are etched in the substrate in a specific portion of the horn aperture, in order to correct the phase of the electromagnetic wave and allow the beam pointing in the desired direction. Moreover, a tapered ladder transition is placed at the horn aperture to improve the impedance matching and enhance the radiation performance. Simulation results prove that the 6 dB bandwidth is wider than 40 GHz in the frequency range $24-64$ GHz. In particular, the same beam pointing is guaranteed over the whole bandwidth with realized gain of 6.4, 8.5 and 8.7 dBi at 28, 38 and 60 GHz respectively. Simulations including two symmetric elements pointing opposite directions and a central element show that the angle of 90° can be covered with peak gain of 7.5 dBi at 28 GHz.**

***Index Terms*—SIW horn antenna, phase correction, wideband, beam pointing, 5G mobile devices.**

I. Introduction

With the development of the fifth generation (5G) mobile communication systems, centimeter and millimeter wave bands are selected in order to satisfy the demand for wider bandwidth to support higher data rates. As a result, the larger free-space path loss, more significant at the higher frequencies, according to the Friis Transmission Equation [1], requires the use of higher gain antennas, affected though by narrow radiation beamwidth. Therefore, the need for new antenna designs that guarantee both high gain and wide coverage is considerably increasing.

Substrate integrated waveguide (SIW) horn antenna is a representative end-fire antenna in millimeter wave band [2]. Characterized by low profile, low cost, light weight, low complexity, ease of fabrication and low insertion loss, it is an attractive candidate because of its strong potential of integration [3] and results a suitable element for the design of beam-steerable directional phased arrays for the new generation mobile devices. However, since the electromagnetic wave phase distribution in the horn aperture is not uniform, due to the severe impedance mismatch between the radiating aperture and free space, SIW horn antennas suffer from low aperture efficiency, that leads to deteriorated radiation performance.

To correct the phase distribution and enhance the gain, the horn antenna proposed in [4] is loaded with rectangular and elliptical shaped dielectric slabs, which act as guiding structures. Tuning their length, it is possible to narrow the beamwidth both in the E-plane and in the H-plane, obtaining thus high gain. A thicker polycarbonate dielectric loading together with metallic strips are adopted in the design presented in [5], with the scope to enlarge the bandwidth and improve the front-to-back ratio. Moreover, metal rectangular patches and dielectric loading are integrated to the aperture of the horn antenna described in [6], which exhibits the advantages of narrow E-plane beamwidth, high gain and reduced sidelobes and backward radiation. Other solutions employ printed transitions after the horn aperture, e.g. the design in [7], where the offset double-sided parallel-strip lines structure proposed in [8] is involved, to give good impedance matching and wide bandwidth. The research effort in [9] proposes symmetric gaps ecthed on the H-plane metallic walls of the SIW horn antenna to overcome the problem related to the electromagnetic field phase distribution. In addition, the tapered-ladder transitions, introduced and optimized by the same authors in [10], [11] are printed at the horn aperture to achieve a better radiation and impedance matching. Another strategy, adopted in [12], consists in realizing a smooth transition from the horn aperture to the free space by perforating air-vias with different diameters into the semi-open horn and allows to achieve a wide bandwidth. Furthermore, the advantages of good impedance matching, high gain of 13.3 dBi and good radiation performance are offered by the two slots etched on the ground of the antenna proposed in [13]. A pair of slots is also exploited in the top and bottom metallization of the SIW horn antenna in [14], with the aim to suppress back lobe radiation, and two additional vias in the waveguide improve significantly the return loss. Some of the afore-mentioned design along with alternative solutions to the bandwidth and gain limitations of the horn antennas are collected in [15], which reviews the development of SIW end-fire antennas in the last fifteen years.

The proposed SIW horn antenna design represents the first attempt to achieve the desired beam pointing through the control of the electromagnetic wave phase distribution in the horn aperture. Air-via technology is adopted for this purpose and air vias are etched in the substrate to address the radiation to a specific direction. Inspired by [9], the optimized tapered ladder transition is placed after the horn aperture, to improve the impedance matching and enhance the radiation performance. The solution allows to obtain stable radiation performance over a wide bandwidth and to satisfy the requirements of wideband, large coverage and high gain of the new generations mobile communication systems. Moreover, simulations including three elements placed in the top edge of the PCB prove that it is possible to cover the angle range of around 90° with high gain.

The paper is organized as follows. First, the main parts of the proposed SIW H-plane horn antenna are described in detail in Section II. Then, in Section III, the performance of the structure in the simulated environment are presented and discussed. Finally, Section IV concludes the paper.

II. Structure of the SIW Horn Antenna

The geometry of the SIW H-plane sectoral horn antenna is given in Fig. 1. The antenna is integrated in a double layer of Rogers RO4003C substrate, with dielectric constant $\varepsilon_r = 3.55$ and loss tangent $\delta = 0.0027$. The two substrates have width 40 mm, length 25 mm and thickness 1.524 mm. The other dimensions are listed in Table I. Two flaring rows of metallic vias form the side walls of the SIW horn antenna, that consists of three main parts. The first L_1 section is the waveguide feeding region. To feed the horn antenna, waveguide port is selected for the analytical study conducted using the electromagnetic simulator *CST Microwave Studio 2019*. L_2 represents the length of the flare part. Air vias are etched in the substrate to adjust the electromagnetic wave phase distribution, in order to direct the main beam to the desired direction. Finally, the clearance L_c corresponds to the tapered ladder transition, printed on the top side of the PCB, to achieve a better impedance matching and improve the radiation performance. The optimized transition, made up of 23 scaled triangles spaced 0.6 mm, allows to minimize the clearance to 3 mm.

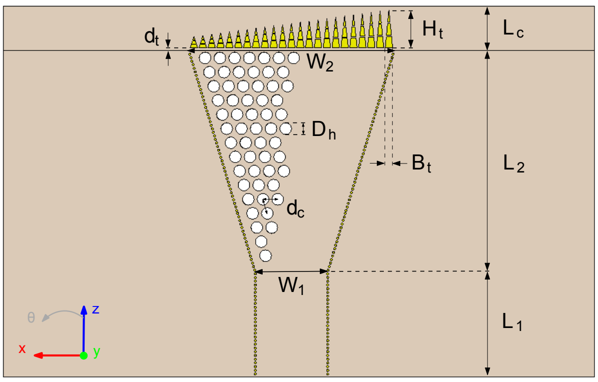

Fig. 1. Geometric structure and parameters of the proposed SIW horn antenna.

Tab. I. Dimensions of the SIW horn antenna parameters (units: mm).

Parameter	Value	Parameter	Value
L_c	3	D_h	0.8
L_1	7	d_c	1
L_2	15	H_t	2.5
W_1	5	B_t	0.5
W_2	14	d_t	0.2

III. SIW Horn Antenna Performance

In the simulated model the two rows of metallic vias are simplified to metal walls. The curve representing the S-parameter characteristic of the proposed SIW horn antenna is reported in Fig. 2(a). Wide band performance are shown by the simulated structure. The impedance matching is achieved over the all frequency band considered, resulting in a 6 dB bandwidth wider than 40 GHz. The tapered ladder transition guarantees the good impedance matching between the horn aperture and the free space and enhances the radiation performance.

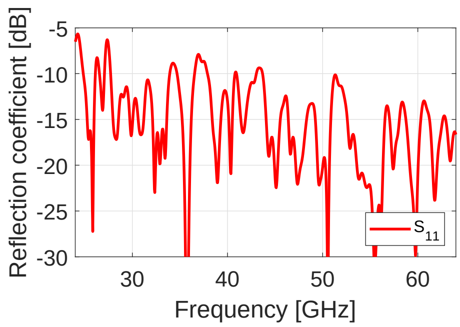

(a)

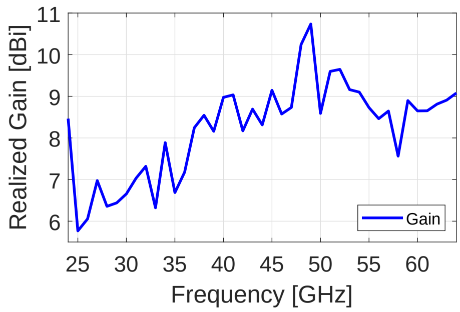

(b)

Fig. 2. (a) Simulated S-parameter characteristic and (b) realized gain of the proposed SIW horn antenna.

The realization of the desired beam pointing is accomplished by controlling the phase velocity of the electromagnetic wave through the etching of air vias in the substrate. In fact, as shown in Fig. 3(b), the presence of air vias in the left side of the horn aperture aims to correct the phase of the E-field in order to allow the propagation in the right side, directing thus the beam to the right portion of the area. Whereas in the design without air vias in Fig. 3(a), the direction of the E-field through the aperture is the same as along the waveguide, since the propagation does not encounter any obstacle. Varying the dimension, density and number of holes in the PCB, it is possible to adjust the phase velocity and consequently achieve a different beam scanning. Moreover, the choice to increase the size of the transition components in the direction of the radiation contributes in ensuring the desired coverage.

Figure 4 shows the 3D radiation characteristics of the proposed antenna at the reference frequency points in mm-wave bands. Comparing the radiation pattern at 28, 38 and

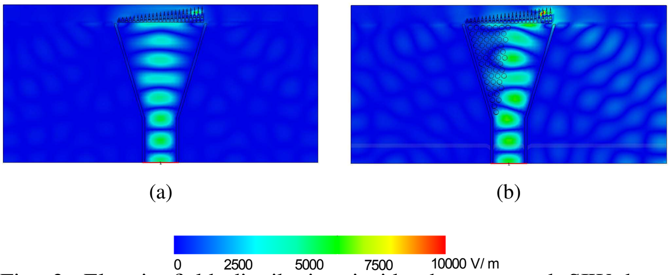

Fig. 3. Electric field distribution inside the proposed SIW horn antenna (a) without and (b) with air vias etched in the substrate.

60 GHz, it is possible to conclude that the optimization of the air vias in the substrate allows to guarantee the same beam pointing over a wide bandwidth. Moreover, Fig. 2(b) highlights that the realized gain is overall above 6 dBi, reaching values higher than 8 dBi when $f > 37$ GHz. In particular, 6.4 dBi is the gain achieved at 28 GHz, 8.5 and 8.7 dBi at 38 and 60 GHz respectively. Finally, the main beam becomes narrower moving up in frequency, as expected.

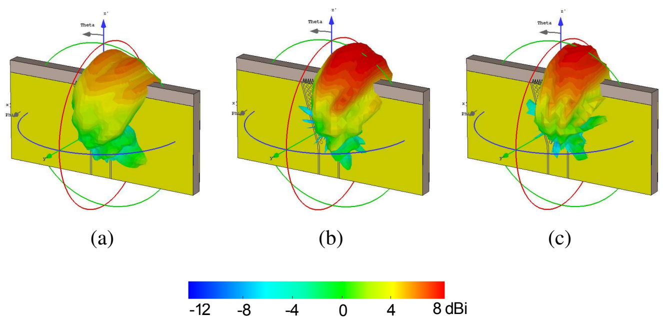

Fig. 4. Simulated radiation pattern of the SIW horn antenna at (a) 28 GHz (b) 38 GHz and (c) 60 GHz.

A. *SIW horn antenna array*

In order to prove that the proposed SIW horn antenna is a suitable candidate for the next generation beam steerable arrays, three elements are placed in the upper edge of the PCB at a distance of 2.8 mm. The width of the substrate in Fig 5 is 70 mm, according to the size of the state-of-the-art mobile devices. The S-parameter characteristics in Fig. 6(a) confirm the wide bandwidth performance and mutual coupling lower than -20 dB, ensured by the chosen minimum distance. The 2D-coverage property of the antenna system at 28 GHz is reported in Fig. 6(b). The curve representing the envelope shows that it is possible to steer the beam of 90°, from $-45°$ to 45°. In particular, each radiating element covers an area of 30° with maximum gain of 7.5 dBi, which results higher than that realized by the single antenna.

IV. Conclusion

This work proposes a new SIW horn antenna for the new generation beam steerable arrays. The main purpose of the design is to obtain stable radiation performance over a wide bandwidth and is achieved through the use of air vias etched in the substrate and a tapered ladder transition placed at the horn aperture. The first allows to control the phase velocity of the electromagnetic wave propagating along the horn aperture and address the main beam to a specific direction. The second ensures a good impedance matching in the transition between horn aperture and free space, improving also the radiation performance. The component is characterized by the same beam pointing over the whole simulated bandwidth $24-64$ GHz, with realized gain increasing from 6 to 9 dBi on average moving up in frequency. Moreover, placing three elements in the top edge of the PCB allows to cover the angle of 90° with peak gain of 7.5 dBi at 28 GHz. Future work aims to reduce the dimensions of the proposed structure, in order to optimize the space occupied on the PCB, and to investigate a solution to increase the gain at the lower frequencies. The following step consists in exploiting the enhanced element in the design of an antenna array that covers the 3D full sphere with high gain over a wide bandwidth.

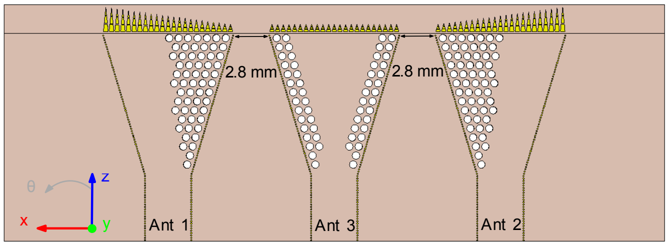

Fig. 5. Design of the proposed beam-steerable SIW horn antenna array for 5G mobile-phones.

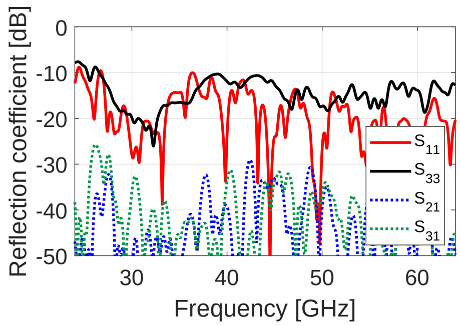

(a)

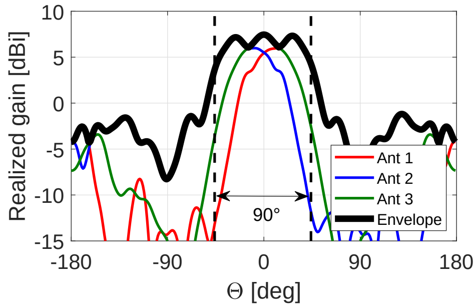

(b)

Fig. 6. (a) Simulated S-parameter characteristics and (b) spherical coverage at 28 GHz of SIW horn antenna array. Due to the symmetric structure, S_{22} and S_{32} are omitted here.

Acknowledgments

The work presented in this paper has been conducted under the framework of the RANGE project, supported by The Innovation Fund Denmark together with industry partners: WiSpry, AAC and Sony Mobile.

References

[1] C. A. Balanis, *Antenna theory: analysis and design*. John wiley & sons, 2016.

[2] Z. Li, K. Wu, and T. A. Denidni, "A new approach to integrated horn antenna," in *2004 10th International Symposium on Antenna Technology and Applied Electromagnetics and URSI Conference*, pp. 1–3, IEEE, 2004.

[3] Y. Cassivi, L. Perregrini, P. Arcioni, M. Bressan, K. Wu, and G. Conciauro, "Dispersion characteristics of substrate integrated rectangular waveguide," *IEEE Microwave and Wireless components letters*, vol. 12, no. 9, pp. 333–335, 2002.

[4] H. Wang, D.-G. Fang, B. Zhang, and W.-Q. Che, "Dielectric loaded substrate integrated waveguide (siw) h-plane horn antennas," *IEEE Transactions on Antennas and Propagation*, vol. 58, no. 3, pp. 640–647, 2010.

[5] M. Yousefbeiki, A. A. Domenech, J. R. Mosig, and C. A. Fernandes, "Ku-band dielectric-loaded siw horn for vertically-polarized multi-sector antennas," in *2012 6th European Conference on Antennas and Propagation (EUCAP)*, pp. 2367–2371, IEEE, 2012.

[6] L. Gong, K. Y. Chan, and R. Ramer, "Substrate integrated waveguide h-plane horn antenna with improved front-to-back ratio and reduced side-lobe level," *IEEE Antennas and Wireless Propagation Letters*, vol. 15, pp. 1835–1838, 2016.

[7] Y. Cao, Y. Cai, C. Jin, Z. Qian, L. Zhu, and W. Zhang, "Broadband siw horn antenna loaded with offset double-sided parallel-strip lines," *IEEE Antennas and Wireless Propagation Letters*, vol. 17, no. 9, pp. 1740–1744, 2018.

[8] H. Xu, Y. Li, D. Ye, and Y. Long, "A broadband offset-parallel-parallelograms printed endfire antenna," *IEEE Antennas and Wireless Propagation Letters*, vol. 16, pp. 1167–1170, 2017.

[9] L. Wang, M. Esquius-Morote, X. Yin, and J. R. Mosig, "Gain enhanced h-plane gap siw horn antenna with phase correction," in *2015 9th European Conference on Antennas and Propagation (EuCAP)*, pp. 1–5, IEEE, 2015.

[10] M. Esquius-Morote, B. Fuchs, J.-F. Zürcher, and J. R. Mosig, "A printed transition for matching improvement of siw horn antennas," *IEEE Transactions on Antennas and propagation*, vol. 61, no. 4, pp. 1923–1930, 2013.

[11] M. Esquius-Morote, B. Fuchs, J.-F. Zürcher, and J. R. Mosig, "Novel thin and compact h-plane siw horn antenna," *IEEE Transactions on Antennas and Propagation*, vol. 61, no. 6, pp. 2911–2920, 2013.

[12] Y. Cai, Y. Zhang, L. Yang, Y. Cao, and Z. Qian, "A low-profile wideband surface-mountable substrate-integrated waveguide horn antenna," *IEEE Antennas and Wireless Propagation Letters*, vol. 16, pp. 2730–2733, 2017.

[13] M. Asaadi and A. Sebak, "Broadside high gain h-plane substrate integrated horn antenna for future 5g applications," in *2016 IEEE International Symposium on Antennas and Propagation (APSURSI)*, pp. 1491–1492, IEEE, 2016.

[14] Y. Luo and J. Bornemann, "Substrate integrated waveguide horn antenna on thin substrate with back-lobe suppression and its application to arrays," *IEEE Antennas and Wireless Propagation Letters*, vol. 16, 2017.

[15] Y. Cao, Y. Cai, L. Wang, Z. Qian, and L. Zhu, "A review of substrate integrated waveguide end-fire antennas," *IEEE Access*, vol. 6, pp. 66243–66253, 2018.